14th International Conference on Structural Safety and Reliability - ICOSSAR'25
1-6 June, 2025 - Los Angeles California, USA
R. Ghanem, E. Johnson, S. Masri and A. Olivier (Eds)

ACCESSIBILITY RISK ASSESSMENT UNDER CASCADIA SUBDUCTION ZONE EARTHQUAKES: CASE STUDY ON HOSPITAL ACCESSIBILITY IN PORTLAND METRO AREA

Anteneh Z. Deriba[1] and David Y. Yang[2]

[1]Department of Civil and Environmental Engineering, Portland State University
1930 SW 4th Avenue, Portland, Oregon, USA
E-mail: azewdu@pdx.edu

[2] Department of Civil and Environmental Engineering, Portland State University
1930 SW 4th Avenue, Portland, Oregon, USA
E-mail: david.yang@pdx.edu

Key words: Performance-based risk assessment, Bridge fragility modeling, TMCMC sampling, Asset prioritization, Seismic vulnerability analysis

Abstract. *A resilient transportation network is critical for maintaining access to emergency services following natural disasters. This study quantifies hospital accessibility risk in Portland Metro Area from a magnitude 9 Cascadia Subduction Zone earthquake scenario. The transportation network is modeled as a graph consisting of 1,756 nodes and 2,639 links, including 664 bridges located on 461 of the links. Accessibility is measured using Hansen-based metric, and indirect risk is quantified as the expected loss in accessibility resulting from bridge failures. To efficiently estimate network risk and identify critical assets, a Transitional Markov Chain Monte Carlo sampling framework is employed. The results indicate that the analyzed earthquake scenario could cause an approximately 12% loss in hospital accessibility. Additionally, fragility models with two different levels of complexity were investigated to demonstrate the effects of fragility simplification on (a) the network-level risk and (b) the ranking of critical links. The comparison reveals that an overly simplistic fragility model may underestimate the network-level risk by about 31%, and it may also deliver drastically different rankings for critical links.*

1 INTRODUCTION

Performance indicators such as network connectivity, efficiency, flow capacity, and travel cost have been widely employed in prior studies to evaluate the functionality and vulnerability of transportation networks (Rivera-Royero et al. 2022). While these metrics provide insights into the overall performance of the network, accessibility has gained particular attention in recent years for its ability to capture user-centered impacts (Negm et al. 2025), especially following extreme events. In the aftermath of earthquakes, accessibility to critical services such as hospitals becomes a decisive measure of the network's performance in supporting emergency response and recovery efforts. Accessibility metrics account for both the spatial arrangement of service locations and the impedance or travel cost required to reach them, making them suitable for assessing functionality risk of transportation systems (Chang and Nojima 2001; Sohn 2006; Taylor and Susilawati 2012).

Quantifying risk using performance indicators requires evaluating both the probability and consequence of system failure scenarios. For large-scale networks, the number of possible scenarios grows exponentially with the number of assets. This makes full enumeration computationally infeasible. In addition, scenarios with low probability but high consequences may dominate system risk. These scenarios are likely to be missed by conventional Monte Carlo sampling approaches. To address this, a Transitional Markov Chain Monte Carlo (TMCMC) framework was introduced in the authors' previous work (Deriba and Yang 2025). By leveraging TMCMC, both network-level risk and the importance of an asset to the overall risk can be efficiently determined, even for State-level transportation networks.

Estimating asset failure probabilities requires knowledge of their capacities, typically characterized by fragility curves. These curves relate seismic intensity measures to the probability of damage and are often developed through analytical or empirical methods (Alam and Billah 2015). Widely used models such as those adopted in HAZUS rely on broad classifications that do not adequately differentiate between individual bridges in a network, often overlooking structural and geometric variations (Padgett and DesRoches 2008). While HAZUS fragility models provide a practical basis for regional assessments, they represent standardized archetype structures rather than detailed site-specific behavior. More detailed fragility models, developed through refined structural analysis or updated empirical data, can capture variations that significantly affect risk estimates at the system level. Understanding when and how simplifications in fragility modeling impact overall risk assessments remains an important open question. This study investigates the implications of fragility model generalization on accessibility-based risk assessment by comparing risk assessment outcomes derived from different fragility modeling strategies.

In this study, the transportation network of the Portland Metro Area is used as the case study for evaluating accessibility risk under a Cascadia Subduction Zone (CSZ) earthquake scenario. The network is constructed from primary arterial roads and designated emergency response routes, providing a representative system for assessing post-disaster accessibility. This setting offers a relevant context to examine how seismic events can disrupt connectivity and reduce access to critical services such as hospitals. Details regarding the network modeling, selection of the earthquake scenario, and fragility modeling schemes are presented in the following sections.

2 NETWORK RISK ASSESSMENT OF TRANSPORTATION SYSTEMS

2.1 Graph Model of Transportation Network

In this study, the transportation network is modeled as a graph

$$G = (\mathcal{V}, \mathcal{E}), \tag{1}$$

where $\mathcal{V}$ = the set of nodes representing intersections, and $\mathcal{E}$ = the set of links representing road segments between these nodes. Some of these links contain one or more bridges, which are the primary vulnerable elements in the network and referred to herein as bridge links. Note that the terms "network" and "graph" are used interchangeably in this study. For the purposes of accessibility assessment, nodes in the graph are further classified into two subsets: (1) the subset of population nodes, $\mathcal{P}$, consisting of nodes nearest to one or more census tract centroids, and (2) the subset of hospital nodes, $\mathcal{H}$, consisting of nodes nearest to one or more hospitals. The

proximity is determined based on the geodesic distance, because the centroids and hospital locations normally do not coincide with the network nodes (thus making computing network distance impossible). Some network nodes may be closest to both a hospital and a census tract centroid. In this case, the accessibility of the census tract to the hospital reduces to the accessibility of a network node to itself, which cannot be reasonably estimated with the network model. Hence, whenever such cases arise, the accessibility of a node to itself is excluded from the calculation of accessibility.

For the Portland Metro Area, both primary arterial roads and designated emergency response routes, as defined by Oregon Metro (Oregon Metro 2025), are considered to create the graph model. The resulting network consists of 1,756 nodes and 2,639 links. Among these, 461 links are identified as bridge links, each containing one or more bridges, with a total of 664 bridges covered by the bridge links. Bridges are assigned to links based on spatial alignment between bridge locations and road segments in the network. The network also includes 18 hospital nodes corresponding to the region's healthcare facilities and 614 population nodes aggregating populations in communities across 1,619 census tracts. Since multiple census tracts may be mapped to the same nearest node, the number of population nodes is smaller than the number of tracts. Figure 2 shows the constructed network and the spatial distribution of bridge links, population nodes, and hospital nodes.

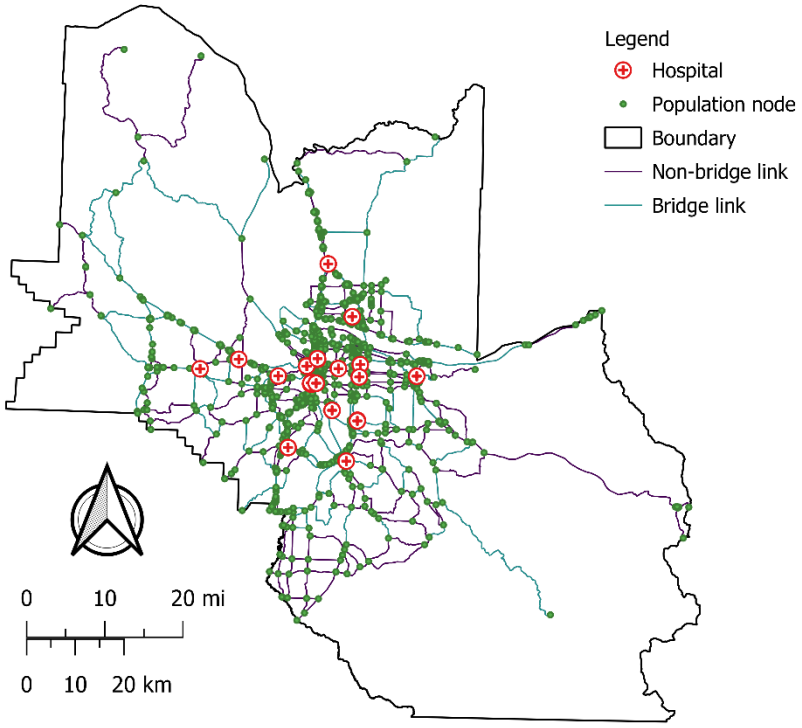

Figure 1: Map of Portland Metro Area Network

2.2 Indicator for Network Accessibility

Accessibility-based performance indicators have been widely employed to quantify the functionality impact of network disruptions. These indicators evaluate how easily populations can reach essential services, particularly during emergencies. Several categories of accessibility

measures exist in the literature. Methods such as the floating catchment area and the accessibility/remoteness index use binary thresholds to define catchment areas around services, assuming full access within a fixed radius and none beyond (Luo and Wang 2003; Taylor et al. 2006). More refined approaches, such as the enhanced two-step floating catchment area method (Luo and Qi 2009), introduce stepwise distance decay functions and incorporate supply-demand balance. However, these methods suffer from limitations due to abrupt cutoffs and the subjective assignment of distance thresholds for accessibility calculation.

In this study, a simplified yet interpretable version of the Hansen integral accessibility index (Hansen 1959) is adopted. The original Hansen index computes accessibility using a weighted sum of service opportunities discounted by distance. Here, identical service capacities are assumed for all the hospital nodes, and a reciprocal distance function is used. Specifically, the accessibility of a population node $\mathrm{i} \in \mathcal{P}$ is defined as the average of the reciprocal shortest-path distances to all hospital nodes, excluding itself if $\mathrm{i} \in \mathcal{H}$. Mathematically, the accessibility of a population node i is given by:

$$\mathrm{A_i} = \frac{1}{|\mathcal{H}_{\sim \mathrm{i}}|} \sum_{j \in \mathcal{H}_{\sim \mathrm{i}}} \frac{1}{\mathrm{d_{ij}}}, \quad \forall i \in \mathcal{P} \tag{2}$$

where d_{ij} = the shortest distance between population node i to hospital node j, $\mathcal{H}_{\sim \mathrm{i}}$ = the set of hospital nodes excluding node i if it is also a hospital node. To evaluate network-level performance, the accessibility values of all population nodes are aggregated within the network:

$$A_{NET} = \sum_{i \in \mathcal{P}} A_i \tag{3}$$

This measure captures cumulative ease, with which the population can reach healthcare services. It is sensitive to increases in travel distance caused by infrastructure disruptions, particularly bridge failures, and reflects the functional consequences of these disruptions. It should be noted that the proposed accessibility index assumes equal "attractiveness" among all hospitals. Given more details of the hospitals (which are not available to the authors at the moment), the attractiveness of a hospital could be quantified, e.g., based on average waiting time (Ugwu et al. 2022), and incorporated into the accessibility index.

2.3 Network Accessibility Risk

During and after a hazard event such as an earthquake, bridge failures can significantly reduce accessibility by increasing the travel distance between population nodes and hospital nodes. Therefore, the indirect risk of a transportation network can be defined as the expected loss in accessibility, expressed as follows:

$$\rho_{NET} = \sum_{s} p(\mathbf{s}) \cdot \left| A_{NET,0} - A_{NET}(\mathbf{s}) \right| \tag{4}$$

where $\mathbf{s}$ = vector representing the survival/failure states of bridge links, $p(\mathbf{s})$ = probability of the system state, and $A_{NET}(\mathbf{s})$ and $A_{NET,0}$ = network accessibility values given a system state $\mathbf{s}$ and that without any bridge failure, respectively.

To compute these accessibility metrics given bridge failure, bridge fragility and detour data are integrated into the network model. Bridge characteristics are obtained from the Federal

Highway Administration's (FHWA) InfoBridge database (FHWA 2024) which provides the parameters needed to define fragility (elaborated in subsequent Section 3.2). Each bridge is associated with a predefined detour length, also extracted from the FHWA InfoBridge database. It is assumed that this detour relies on local roads that are not included by the network model.

Since a single bridge link may contain multiple bridges, the failure probability of a bridge link is calculated by assuming independent failure of bridges on the link. To translate bridge failure probabilities into link failure probabilities, each bridge link is assumed to fail if any of its constituent bridges fail. Therefore, the failure probability of a bridge link l is computed as:

$$p_l = 1 - \prod_{i \in \mathcal{B}_l} (1 - p_i) \tag{5}$$

where $\mathcal{B}_\ell$ = the set of bridges located on link l, and p_i= the failure probability of bridge i. In addition, if a bridge link fails, the corresponding detour length is determined conservatively by adding detour lengths of all bridges on the link. As shortest-path distances increase due to detours, the resulting accessibility values decrease, thereby capturing the functional impact of bridge failures on healthcare access.

To estimate this risk efficiently, the Transitional Markov Chain Monte Carlo (TMCMC) framework is employed. Originally developed for Bayesian updating, TMCMC is a sequential sampling method that can estimate the normalization constant (or evidence) of high-dimensional posterior distributions. In the context of risk assessment, the network risk can be formulated to the evidence term in Bayesian updating (Deriba and Yang 2025), thereby enabling the use of TMCMC for risk assessment.

Specifically, the TMCMC method initiates link failure samples from the prior distributions. A stage-by-stage sampling protocol sequentially samples link failures that are most relevant to quantifying the network risk. This includes rare but high-consequence system states, which conventional Monte Carlo simulation struggles with. As a result, TMCMC offers an efficient means to quantify indirect risk even in large and complex networks. In addition to estimating network risk, the link failure samples in the last stage can be used to measure asset importance. These importance measures of links can support targeted decision-making for risk mitigation. For a detailed description of the methodology, the reader is referred to Deriba and Yang (2025).

3 CSZ EARTHQUAKES AND BRIDGE FAILURE PROBABILITIES

3.1 Seismic Hazard

To characterize the seismic hazard, ground motion intensity measures are obtained from broadband synthetic seismogram simulations developed under the M9 Project, which models magnitude 9 CSZ earthquakes (Frankel et al. 2018; Wirth et al. 2018). This dataset includes 30 distinct rupture scenarios, each representing a plausible variation in slip distribution, rupture dynamics, and source location along the subduction interface. For each scenario, spectral acceleration values at multiple periods are provided over a spatial grid covering the Portland Metro Area.

Based on HAZUS Technical Manual (FEMA 2024), the spectral acceleration at 1-second period (Sa-1s) is used as the intensity measure for evaluating bridge fragility and the associated probability of bridge failure. For each of the 30 simulation scenarios, a unique spatial field of Sa-1s is available in a gridded format. To obtain ground motion estimates at bridge locations, cubic spline interpolation is applied to the gridded Sa-1s values, producing a continuous surface from which site-specific Sa-1s values can be extracted for all bridges. Considering all 30 scenarios, each bridge is assigned 30 distinct Sa-1s values, one from each scenario. Later in Section 3.3, a method is presented to select the most critical scenarios among the 30 scenarios.

3.2 Bridge Fragility Models

Two types of fragility models are considered in this study to investigate the effect of fragility modeling on network risk assessment and risk-based asset ranking. The first strategy uses the fragility models prescribed in the HAZUS Technical Manual (FEMA 2024), which remains widely used for regional bridge risk assessments. In this approach, each bridge is assigned to one of the 28 HAZUS bridge classes based on structural characteristics extracted from the FHWA InfoBridge database. Each class has an associated "standard" fragility curve that defines the probability of reaching or exceeding a given damage state as a function of Sa-1s based on the cumulative distribution function (CDF) of a lognormal distribution. These standard curves are parameterized by a median value and a dispersion factor. The median value of a standard curve is further modified to account for bridge-specific attributes such as skew angle, foundation type, and abutment behavior (FEMA 2024). Among the four damage states considered in HAZUS, only the complete damage state is used to quantify bridge failure probability. In particular, the Sa-1s value at each bridge is used as input of the complete damage fragility curve to compute the probability of bridge failure. In addition to this HAZUS fragility curves, a second strategy is implemented to intentionally further simplify the fragility model. In this approach, a single curve termed as homogenized fragility curve is applied uniformly to all bridges in the network, disregarding individual bridge characteristics. This homogenized fragility curve is constructed by using the median value of the median parameters from all bridges obtained with the HAZUS method. The same dispersion factor of 0.6 is adopted. The resulting fragility curve is shown in Figure 2, overlaid on top of the HAZUS fragility curves used in the baseline model. The network risk and risk-based bridge link ranking, evaluated using the homogenized fragility curve, are compared with those obtained using the baseline HAZUS fragility curves.

The comparison between HAZUS and homogenized fragility models aims to highlight the effect and implications of fragility simplification. As can be expected, if the network risk were a simple sum of asset risks (as in the case of direct economic risk), the effect of using an overly simplified fragility model, e.g., the homogenized fragility curve, might be negligible due to compensating over- and underestimations. However, accessibility is a network performance indicator nonlinear with respect to the link failure probabilities. As such, oversimplifying fragility models may lead to biased estimates of network-level risk and distorted identification of critical assets.

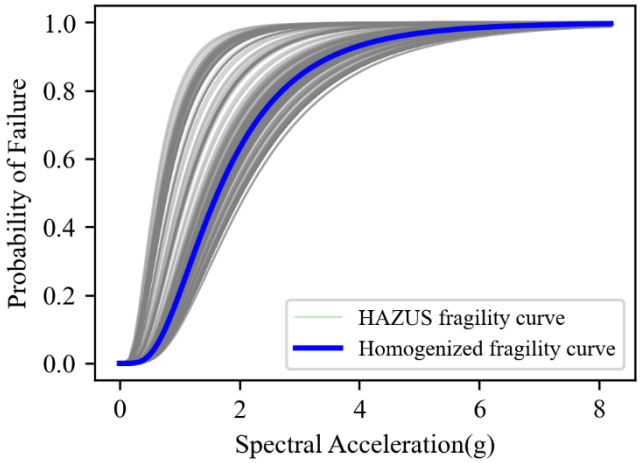

Figure 2: HAZUS curves of all PDX bridges and the corresponding homogenized fragility curve

3.3 Scenario Selection

As described earlier, the ground motion dataset consists of 30 distinct CSZ earthquake scenarios, each with a plausible Sa-1s field. Because ground shaking intensity and spatial distribution vary across these scenarios, the expected damage and accessibility loss also differ among scenarios. To select the worst-case scenario for risk assessment, a selection approach is applied. Specifically, for each bridge, the failure probability is computed for all 30 scenarios using the HAZUS fragility curve described previously. The scenario that results in the highest failure probability is recorded for that bridge. The scenario that is recorded by a majority of all bridges is identified as the worst-case scenario. Following this procedure, the scenario labeled csz009 is selected from the 30 scenarios. Figure 3 shows the spatial distribution of Sa-1s field in this scenario. This scenario is then used in accessibility risk assessment and fragility investigation, presented in the remainder of this paper.

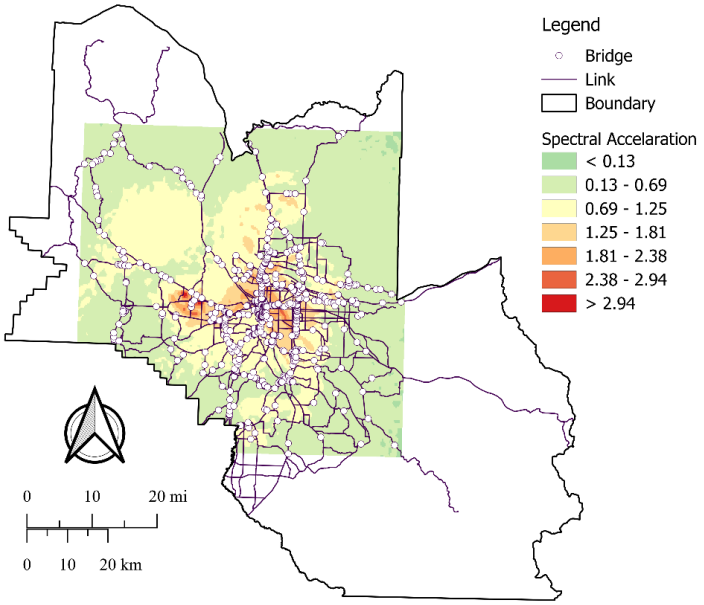

Figure 3: Sa-1s field created for scenario csz009

4 RESULTS AND DISCUSSION

4.1 Results of Risk Assessment and Link Importance

The indirect risk to hospital accessibility in the Portland Metro Area was evaluated using the TMCMC-based sampling framework under the most detrimental Cascadia Subduction Zone earthquake scenario, selected based on the approach described in Section 3.3. The expected reduction in accessibility, quantified as network-level risk, was 11.6% based on the HAZUS-based fragility models.

In addition to estimating risk at system-level, the TMCMC samples were used to derive importance measures for each bridge link. Following the definition introduced in the authors' previous work (Deriba and Yang 2025), the importance measure α_k for bridge link k is computed as:

$$\alpha_k = \frac{\sum_{j=1}^{N_s} s_{jk}^{(-1)}}{N_s} \tag{6}$$

where N_s= the number of TMCMC samples in the final stage, and $s_{jk}^{(-1)}$ = binary damage state of bridge link k in sample j. This measure corresponds to the posterior failure frequency of the asset under risk-informed sampling and captures both likelihood and consequence in a single metric.

Bridge links with high importance values either have a high likelihood of failure, a great impact on accessibility, or both. These values support rational prioritization of assets for retrofitting and risk mitigation. Figure 4 shows the spatial distribution of bridge link importance across the Portland network. High-importance links are concentrated along major corridors such as I-5, I-84, and I-405, reflecting both structural vulnerability and their central role in maintaining hospital access under seismic disruption.

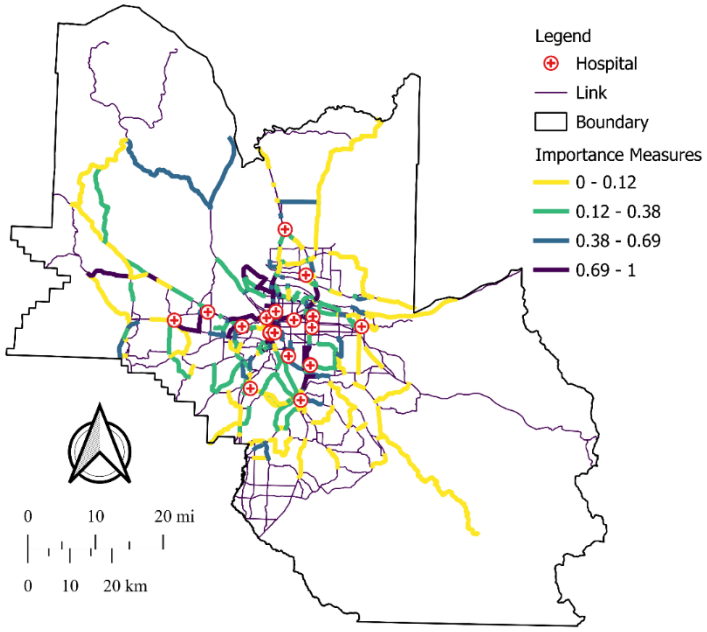

Figure 4: Map of bridge link importance measures (HAZUS fragility curves)

4.2 Effect of Fragility Simplification

To evaluate the influence of fragility modeling assumptions on network-level risk and asset prioritization, the analysis is repeated using the homogenized fragility curve, introduced in Section 3.2 and shown in Figure 2. In particular, this analysis replaced the bridge-specific HAZUS fragility curves with a single generalized curve applied uniformly across all bridges in the network. While this simplification significantly reduces input complexity, it also removes the variability in structural capacity and damage susceptibility among individual bridges.

The repeated risk assessment revealed that fragility model simplification leads to a significant underestimation of indirect risk from 11.6% using the detailed HAZUS fragility curves to 8% using the single homogenized fragility curve. This amounts to a 31% reduction with respect to the estimated risk. This decrease highlights the sensitivity of accessibility-based risk metrics to assumptions made about asset-level fragility.

In addition, and perhaps more importantly, asset importance measures and the corresponding asset ranking were also affected due to the use of the homogenized fragility curve. To quantify the effect on asset ranking, Spearman's rank correlation coefficient was calculated between the importance measures derived from the two types of fragility models (i.e., HAZUS vs. homogenized). When all bridge links in the network were considered, the correlation was 0.86, indicating moderate consistency in the overall ranking. However, infrastructure decision-makers are typically most concerned with identifying the most critical assets for targeted interventions. When only the top 25% of bridge links was compared by importance, the correlation dropped to 0.62. For the top ten most critical bridge links, the correlation declined further to 0.30. This trend demonstrates that fragility simplification can distort the identification of high-priority assets.

Table 1: Top 10 most critical bridges identified using HAZUS fragility curves vs. the homogenized fragility curve

Rank	HAZUS Fragility Curves		Homogenized Fragility Curve	
	Link ID	**Road Name**	**Link ID**	**Road Name**
1	89	I-405 b/n Burnside St and SW Taylor St	78	I-405 b/n SW Clay St and SW Taylor St
2	124	I-5 b/n Burnside St and SE Washington St	170	NW Cornell Rd b/n NW Saltzman Rd and NW 23rd
3	170	NW Cornell Rd b/n NW Saltzman Rd and NW 23rd	89	I-405 between Burnside St and SW Taylor St
4	78	I-405 between SW Clay St and SW Taylor St	380	I-5 between N Marine Dr and Lewis and Clark Hwy
5	118	I-84 b/n NE 39th Ave and NE 82nd Ave	115	I-205 (Southbound) b/n SE Sunnyside Rd and SE Foster Rd
6	100	I-84 b/n NE 16th Ave and NE Sandy Blvd	194	I-205 (Northbound) b/n SE Sunnyside Rd and SE Foster Rd
7	101	I-5 b/n SE Washington St and Morrison St	26	I-405 b/n SE 4th Ave and SW Broadway
8	380	I-5 b/n N Marine Dr and Lewis and Clark Hwy	27	SE Tacoma St b/n SE McLoughlin Blvd and SE 32nd Ave
9	194	I-205 (Northbound) b/n SE Sunnyside Rd and SE Foster Rd	250	SE Cornelius Pass Rd b/n SW Taulatin Valley Hwy and NE Walker Rd
10	115	I-205 (Southbound) b/n SE Sunnyside Rd and SE Foster Rd	124	I-5 b/n Burnside St and Morrison St

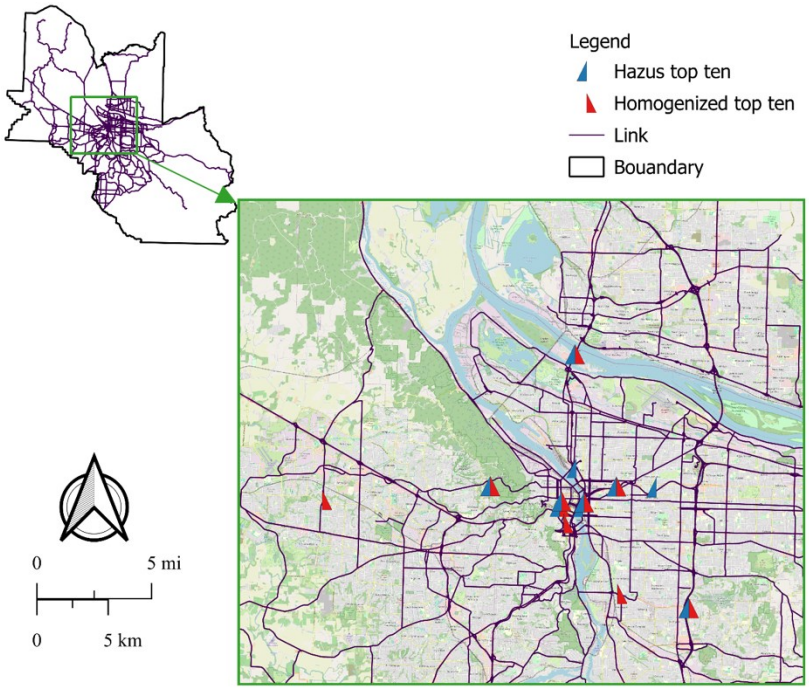

Figure 5: Top 10 bridge links under the HAZUS fragility curves vs. homogenized fragility curve

Table 1 lists the top ten bridge links obtained using both types of fragility models. Although seven links appear in both lists, their relative positions vary significantly. Figure 5 visualizes these top ten assets on the transportation network. It should be noted that the map alone does not fully convey the ranking mismatch. Table 1 and Figure 5 together depict a better picture, where some high-ranking assets under the HAZUS fragility curves are demoted or missed entirely under the simplified homogenized fragility curve.

These findings address the broader question posed in the introduction: how the simplifications in fragility modeling affect system-level risk and decision making. The results demonstrate that a generalized fragility curve, while convenient, can underestimate accessibility loss and misrepresent asset importance. Even the standard HAZUS archetypes may be too coarse to reflect the true variability in bridge performance. Preserving asset-specific fragility detail is essential when accessibility metrics are used to inform risk mitigation priorities. Future research should aim to establish thresholds where simplification remains acceptable and to develop criteria that balance model granularity with decision relevance.

5 CONCLUSIONS

This study presents a comprehensive framework for indirect risk assessment of transportation networks, focusing on post-earthquake hospital accessibility. The method integrates a graph-based representation of the Portland Metro Area transportation network with a performance-based risk formulation that quantifies the expected loss in accessibility. A Transitional Markov Chain Monte Carlo (TMCMC) approach is employed to efficiently explore the high-dimensional space of bridge link failure states, enabling accurate estimation of indirect network risk and identification of critical transportation assets. The results demonstrate that a major Cascadia Subduction Zone earthquake can significantly reduce access

to healthcare services. Additionally, the study investigates the importance and implications of fragility model fidelity in the context of risk assessment and risk-based asset prioritization. The main conclusions are summarized below:

- Compared to pre-earthquake performance, a magnitude 9 CSZ earthquake scenario may result in a 11.6% reduction in hospital accessibility across the Portland area network, measured in terms of the adapted Hansen accessibility index. This reflects a significant disruption in the ability of communities to reach healthcare services in the aftermath of a major earthquake.
- The TMCMC-based sampling approach provides an efficient means of evaluating network risk without exhaustively enumerating all possible failure combinations. It also yields risk-informed importance measures for each bridge link. The latter represent the contribution of the assets to the system-level accessibility loss. These measures offer a rational basis for retrofitting prioritization and resource allocation.
- Using a single homogenized fragility curve resulted in a 31% underestimation in the accessibility risk. More importantly, it altered the prioritization of critical bridge links. The changing ranking is more salient among more critical bridge links, as reflected by the decreasing Spearman's rank correlation coefficients among importance measures obtained from both types of fragility models for more and more critical subsets of bridge links.

REFERENCES

[1] Alam, M. S., and AHM. M. Billah. 2015. “Seismic fragility assessment of highway bridges: a state-of-the-art review.” Structure and Infrastructure Engineering, 11 (6): 804–832. Taylor & Francis. https://doi.org/10.1080/15732479.2014.912243.

[2] Chang, S. E., and N. Nojima. 2001. “Measuring post-disaster transportation system performance: the 1995 Kobe earthquake in comparative perspective.” *Transportation Research Part A: Policy and Practice*, 35 (6): 475–494. https://doi.org/10.1016/S0965-8564(00)00003-3.

[3] Deriba, A. Z., and D. Y. Yang. 2025. “Performance-Based Risk Assessment for Large-Scale Transportation Networks Using the Transitional Markov Chain Monte Carlo Method.” *ASCE-ASME Journal of Risk and Uncertainty in Engineering Systems, Part A: Civil Engineering*, 11 (1): 04024090. American Society of Civil Engineers. https://doi.org/10.1061/AJRUA6.RUENG-1402.

[4] FEMA. 2024. “Hazus 6.1 Inventory Technical Manual.” Federal Emergency Management Agency.

[5] FHWA. 2024. “Long-Term Bridge Performance (LTBP) InfoBridge.” *Federal Highway Administration*. Accessed January 1, 2025. https://infobridge.fhwa.dot.gov.

[6] Frankel, A., E. Wirth, N. Marafi, J. Vidale, and W. Stephenson. 2018. “Broadband Synthetic Seismograms for Magnitude 9 Earthquakes on the Cascadia Megathrust Based on 3D Simulations and Stochastic Synthetics, Part 1: Methodology and Overall Results.” *Bulletin of the Seismological Society of America*, 108 (5A): 2347–2369.

[7] Hansen, W. G. 1959. “How Accessibility Shapes Land Use.” *Journal of the American Institute of Planners*, 25 (2): 73–76. Routledge.

[8] Luo, W., and Y. Qi. 2009. “An enhanced two-step floating catchment area (E2SFCA) method for measuring spatial accessibility to primary care physicians.” *Health Place*, 15 (4): 1100–1107. Oxford: Elsevier Sci Ltd.
[9] Luo, W., and F. Wang. 2003. “Measures of Spatial Accessibility to Health Care in a GIS Environment: Synthesis and a Case Study in the Chicago Region.” *Environmental Planning B: Planning and Design*, 30 (6): 865–884. SAGE Publications Ltd STM.
[10] Negm, H., J. De Vos, F. Pot, and A. El-Geneidy. 2025. “Perceived accessibility: A literature review.” *Journal of Transport Geography*, 125: 104212.
[11] Oregon Metro. 2025. “Regional Land Information System Open Database.” Accessed January 7, 2025. https://rlisdiscovery.oregonmetro.gov/.
[12] Padgett, J. E., and R. DesRoches. 2008. “Methodology for the development of analytical fragility curves for retrofitted bridges.” *Earthquake Engineering & Structural Dynamics*, 37 (8): 1157–1174. https://doi.org/10.1002/eqe.801.
[13] Rivera-Royero, D., G. Galindo, M. Jaller, and J. Betancourt Reyes. 2022. “Road network performance: A review on relevant concepts.” *Computers & Industrial Engineering*, 165: 107927. https://doi.org/10.1016/j.cie.2021.107927.
[14] Sohn, J. 2006. “Evaluating the Significance of Highway Network Links Under the Flood Damage: An Accessibility Approach.” *Transportation Research Part A: Policy and Practice*. https://doi.org/10.1016/J.TRA.2005.08.006.
[15] Taylor, M. A. P. and Susilawati. 2012. “Remoteness and accessibility in the vulnerability analysis of regional road networks.” *Transportation Research Part A: Policy and Practice*, 46 (5): 761–771. https://doi.org/10.1016/j.tra.2012.02.008.
[16] Taylor, M., S. Somenahalli, and G. D’Este. 2006. “Application of Accessibility Based Methods for Vulnerability Analysis of Strategic Road Networks.” *Networks and Spatial Economics*, 6: 267–291. https://doi.org/10.1007/s11067-006-9284-9.
[17] Ugwu, I. A., B. Salarieh, A. M. Salman, L. Petnga, and M. Williams. 2022. “Postdisaster Recovery Planning for Interdependent Infrastructure Systems Prioritizing the Functionality of Healthcare Facilities.” Journal of Infrastructure Systems, 28 (4): 04022038. American Society of Civil Engineers. https://doi.org/10.1061/(ASCE)IS.1943-555X.0000719.
[18] Wirth, E. A., A. D. Frankel, N. Marafi, J. E. Vidale, and W. J. Stephenson. 2018. “Broadband Synthetic Seismograms for Magnitude 9 Earthquakes on the Cascadia Megathrust Based on 3D Simulations and Stochastic Synthetics, Part 2: Rupture Parameters and Variability.” *Bulletin of the Seismological Society of America*, 108 (5A): 2370–2388. https://doi.org/10.1785/0120180029.